Catalysis Today 178 (2011) 172–180

Contents lists available at ScienceDirect

Catalysis Today

journal homepage: www.elsevier.com/locate/cattod

The promoting effect of ceria on Li/MgO catalysts for the oxidative coupling of methane

Liangguang Tang, Doki Yamaguchi, Lisa Wong, Nick Burke, Ken Chiang*

CSIRO Earth Science and Resource Engineering, Clayton, VIC 3168, Australia

ARTICLE INFO

Article history:
Received 20 May 2011
Received in revised form 20 July 2011
Accepted 24 July 2011
Available online 21 August 2011

Keywords:
Ceria promoter
Li/MgO
Oxidative coupling of methane

ABSTRACT

The effects of ceria loading (0.1–6.0 wt%) on the properties of Li/MgO catalysts and on their activities for oxidative coupling of methane (OCM) were studied. The catalysts were characterised by surface area measurement, XRD, XPS, SEM and CO_2 temperature programmed desorption. The catalyst activity study suggested that the addition of 0.5–1.0 wt% ceria improved the methane conversion of Li/MgO catalyst significantly at reaction temperatures below 800 °C with little change in C_2 selectivity compared to un-promoted Li/MgO. Further increases in ceria loading resulted in lower methane conversion and C_2 selectivity. The CH_4 conversion was related to the surface distribution of O^- and O^{2-} on the catalysts. An increase in reaction temperature beyond 800 °C or a decrease in CH_4:O_2 ratio from 7:1 to 3:1 imparted negative effects on the methane conversion and C_2 selectivity of the ceria (0.5 wt%) doped Li/MgO catalyst. All ceria doped catalysts did not show any methane coupling activity in the absence of gaseous oxygen, suggesting that they were ineffective to work with alternate feeds of CH_4 and O_2 (redox) mode. Based on the OCM activity and characterisation results, a new pathway that describes the formation of active sites through the electron transfer between $Ce^{4+}/Ce^{3+}$and Li/MgO was proposed to help explain the improved OCM activity by using ceria doped Li/MgO catalysts.

1. Introduction

The conversion of methane into higher hydrocarbons is an important route for the production of synthetic fuels and chemicals. Of all the approaches, the oxidative coupling of methane (OCM) is one of the few processes that is capable of converting methane into higher hydrocarbons in a single step [1]. Recently, however there has been a revival of interest in this route as evidenced by the "Methane Challenge" program launched by the Dow Chemical Company [2].

A number of metal oxides are considered to be effective catalysts for the OCM process and different active sites based on different oxygen species have been suggested [3]. In brief, the first group of catalysts contains reducible metal oxides, which are able to store and release oxygen cyclically between multiple valence states. These materials are more efficient in terms of their redox kinetics and are suitable for use with alternating feeds of methane and oxygen (known as the redox mode). Some examples are SnO_2–SnO and BiO–Bi where the surface lattice oxygen (O^{2-}) has been proposed to be the active site [4]. The second group of catalysts contains irreducible metal oxides including alkali/alkaline earth metal oxides such as Li/MgO [5] and most rare earth metal oxides [6,7] except those of Pr, Ce and Tb. These catalysts usually require a co-feed of methane and gaseous oxygen. Different surface oxygen species including O_2^-, O_2^{2-} and O^- have been reported to be the active sites and the relative activity of these oxygen species for C_2 formation are found to be $O^- \gg O_2^-$ and $O_2^{2-} > O_2^-$ [3,8]. The last group of catalysts contains both non-reducible and reducible components, including alkali or alkaline-doped transition metal oxides such as Li–Ni–O [9] and perovskite-type catalysts (e.g. $BaCe_{1-x}Gd_xO_{3-\delta}$, $Ba_{0.5}Sr_{0.5}Co_{0.8}Fe_{0.2}O_{3-\delta}$) [10]. For these catalysts, adsorbed molecular oxygen, lattice oxygen or a combination of both have been proposed to be the active oxygen sites responsible for C_2 formation.

The nature of the oxygen species on the catalyst surface has been related to activity and selectivity for C_2 production, which are largely determined by the electronic properties of the solid catalysts [3]. Among all the OCM catalysts investigated, Li/MgO catalysts have often shown higher yields of C_2 hydrocarbons and the defect centres [Li^+O^-] that are formed from the insertion of Li into MgO lattices, is thought to be one of the governing factors responsible for methane activation [5]. However, as noted by Korf et al. [11], the highest yield of C_2 hydrocarbons could only be reached at temperatures above 780 °C for Li/MgO. Therefore, lowering the operating temperature without lowering the yield of C_2 hydrocarbons would reduce running costs and possibly reduce capital costs of the process as well. With the intention to improve both the activities and stabilities of Li/MgO based materials, Korf et al. [12] examined the effects of oxide addition to Li/MgO and found that Sn-modified

* Corresponding author. Tel.: +61 3 95458385; fax: +61 3 95458380.
E-mail address: Ken.Chiang@csiro.au (K. Chiang).

0920-5861/$ – see front matter.
doi:10.1016/j.cattod.2011.07.014

Li/MgO was a promising catalyst and the addition of 0.029 mmol/g Sn to Li/MgO resulted in an decrease of reaction temperature by 78 °C for 90% oxygen conversion. They concluded that the promoting effect was due to the improved adsorption of oxygen in the presence of Sn.

Many rare earth metal oxides also exhibited coupling activity with C_2 selectivity between 30 and 50% [6]. However, the lanthanides Ce, Pr and Tb that have multiple oxidation states are frequently regarded as total oxidation catalysts. They show negligible C_2 selectivity [13] in many OCM processes because they react oxidatively with methyl radicals that are formed from CH_4 activation. This reaction often results in the formation of methoxide species and finally the production of CO_x. However, ceria has been under intense scrutiny as a catalyst and as a catalyst promoter because of its excellent redox properties and its ability to provide oxygen vacancies at the surface and in the lattice associated with the rapid reduction of Ce^{4+} to Ce^{3+} [14]. It was suggested that doping OCM catalysts with rare earth metal oxides, especially ceria, would change the electronic properties of catalysts to improve the catalyst activity of OCM reaction.

Ceria has been reported to be an effective dopant for the OCM reaction [14–20]. Pacheco Filho et al. reported the addition of ceria to a Na/CaO catalyst increased the conversion rate (measured in μmol/m^2-h) of the OCM reaction by a factor of eight [15], and it is believed that the charge transfer processes between cerium ions, O^- and O_2^{2-} peroxide sites were responsible for the increase in activity. Zhang et al. established a correlation between oxygen ion conductivity and C_2 selectivity for the CaO-CeO_2 system. They found that both C_{2+} selectivity and oxygen ion conductivity first increased significantly and then gradually decreased giving a maximum at a Ca content of around 20.0–25.0 at.% [16]. The addition of 5.0 wt% ceria to Mn–Na_2WO_4/SiO_2 also enhanced the dispersion of Na_2WO_4 and increased its activity and stability for the OCM reaction [17]. Dedov et al. found that addition of ceria to lanthana at a loading of 10.0 wt% enhanced the performance of the catalyst and suggested that oxygen could be activated directly to produce O^- species when gaseous oxygen was brought into contact with ceria [18].

Bi et al. [19] first observed that Li/MgO promoted with 2.0 wt% ceria showed a significant increase in C_2 selectivity compared to un-promoted Li/MgO when the coupling reaction was conducted at 700 °C. Bartsch et al. [20] observed a higher yield of C_2 when ceria (50.0 wt%) promoted Li/MgO was used at temperatures above 700 °C. This behaviour was attributed to the promoting effect of ceria in the transport of charges which improved the regeneration of [Li^+O^-] active sites. Recently, Gonçalves et al. [21] found that the addition of 0.5 mol% ceria improved methane conversion and C_2 selectivity of Li/MgO and Na/MgO. They also concluded that the improvement was a result of the enhanced charge transfer from cerium to oxygen ions as well as the transfer of oxygen into the lattice.

The ceria loadings used vary greatly in the literature and the effect of ceria addition on Li/MgO catalyst for the OCM reaction has not been assessed in detail. In this work, the structural properties of Li/MgO promoted with varied concentrations of ceria and its OCM activity at different reaction temperatures and CH_4:O_2 ratios are investigated. A reaction mechanism is also developed to explain the promoting effect of ceria for the OCM reaction.

2. Experimental

2.1. Catalyst synthesis

$Mg(CH_3COO)_2{\cdot}4H_2O$, $LiCH_3COO{\cdot}2H_2O$, and $Ce(NO_3)_3{\cdot}6H_2O$ precursors were used to synthesise the catalysts. A solution containing known amounts of the precursors was stirred and evaporated to dryness. The resulting material was dried at 120 °C overnight and calcined in air at 800 °C for 4 h. The acetate precursors were used in this catalyst synthesis since it has been shown by Choudary et al. that these catalysts displayed good stability and their activity and selectivity remained unchanged over 15 h of operation [22]. The lithium concentration was fixed at 3.5 wt% in all the catalysts prepared as this concentration is reported to be the optimal concentration for Li/MgO catalyst [5]. The effects of ceria were evaluated at concentrations of 0.1, 0.5, 1.0, 2.0, and 6.0 wt% in this study.

2.2. Catalyst characterisation

The surface area of samples was determined by N_2 adsorption at −196 °C using a Micromeritics TriStar 3000. The samples were first degassed at 300 °C under vacuum. X-ray diffraction (XRD) analysis of fresh and used catalyst was performed using a Phillips DW 1130 with a radiation source of Cu Kα (λ = 1.5406 Å). A Zeiss Supratm VP40 scanning electron microscope (SEM), operated at 3.0 kV, was used to examine the morphological properties of catalysts before and after the reaction. X-ray photoelectron spectroscopy (XPS) measurements were performed with an ESCALAB250Xi (Thermo Scientific, UK) with a mono-chromated Al Kα source (energy 1486.68 eV). The distribution of surface oxygen species of the catalysts was derived from XPS data [23].

The basicity of catalyst surface was determined by temperature programmed desorption of CO_2 (CO_2-TPD) using a Micromeritics AutoChem 2950. 100 mg of catalyst was packed in a quartz reactor and heated in a flow of helium while the temperature was increased from room temperature to 800 °C. The temperature was then decreased to 50 °C and CO_2 was allowed to flow through the sample at this temperature for half an hour. After the passage of CO_2, the reactor was purged with helium for half an hour. Finally, the temperature was increased from 50 °C to 800 °C at a heating rate of 10 °C/min in a flow of helium, and held at 800 °C for half an hour. The CO_2 desorbed from this final step was monitored online by a thermal conductivity detector (TCD).

In order to assess the activities of the catalysts in the absence of oxygen, a series of CH_4 pulses was brought into contact with the catalyst and the production of C_2 hydrocarbons was monitored. In brief, 100 mg of the catalyst was packed in a quartz sample tube and was calcined in situ at 750 °C in a flow of 10% O_2/He for 2 h. After oxidation, the reactor was purged with helium for half an hour. Pulses (0.5 ml) of methane (10% CH_4/He) carried in helium (30 ml/min) were sent to react with the catalyst at 750 °C. The gas composition in the outlet was monitored online by using a mass spectrometer (Pfeiffer ThermoStar GSD 301).

2.3. Catalyst activity testing

All catalysts were assessed in a fixed-bed quartz reactor operated at atmosphere pressure. An amount of 450 mg catalyst was placed into the isothermal zone of the reactor with its position fixed by two layers of quartz wool. Quartz rods were inserted to the reactor in order to minimize the internal volume of the reactor and therefore the potential for homogeneous gas phase reactions. Prior to the reaction, the catalyst was heated to the desired temperature under a flow of oxygen. Then argon was passed through the catalyst bed for half an hour to remove any residual oxygen. The reaction was commenced by passing through the catalyst bed a mixture of CH_4/O_2/Ar at 100 ml/min with a specified CH_4:O_2 ratio. The total concentration of CH_4 and O_2 was maintained at 15% in the feed gas in order to prevent excessive heat generation and hence the development of a large temperature gradient in the catalyst bed. The outlet gas composition was analysed by using an online gas chromatograph (Shimadzu GC-2014) with a TCD and a flame ionization detector (FID). Hydrogen was separated from the outlet gas

stream by using a 5A molecular sieve packed column (Alltech) and detected by using the TCD. CO, CO_2, C1–C3 hydrocarbons were separated in a Carboxen-1006 PLOT column (SUPELCO) and quantified by the FID.

3. Results

3.1. Catalyst characterisation

As given in Table 1, the surface area of fresh Li/MgO was 3.5 m^2/g. This value agrees with others that Li^+ incorporation in MgO is generally characterised by relatively low surface areas of the final material [24]. The main cause of this low surface area is due to the high temperature condition required for the calcination step for the decomposition of the lithium salt and for the insertion of Li^+ into the MgO lattice to create active sites. In addition, lithia also facilitates the sintering of oxides at such high temperature [25]. The introduction of ceria to Li/MgO catalysts did not significantly alter the surface area of the material with all the ceria loaded catalysts having surface areas below 5 m^2/g after calcination.

Fig. 1(a) shows the XRD patterns of Li/MgO and ceria doped Li/MgO catalysts after calcination, while Fig. 1(b) plots the diffraction peak of MgO which emerged at around 43° for different catalysts. Although the diffraction peaks for MgO were clearly observed in all samples, no peaks attributed to the Li phase were detected. This suggests that Li ions could possibly be interstitially or substitutionally introduced into the MgO lattice and that no segregated Li species was formed.

Despite the fact that there were no evolution of new diffraction peaks from the Li/MgO sample after the introduction of ceria at 0.1 and 0.5 wt%, the peak intensity of MgO has significantly increased and a noticeable shift of MgO peak to the lower angle end could be clearly observed. For example, the primary MgO peak in Li/MgO observed at 43.2° was shifted to 42.8° and 42.6° for Li/MgO/Ce0.1 and Li/MgO/Ce0.5, respectively (see Fig. 1(b)). The increase in MgO peak intensity suggested that the ceria doping could improve the crystallinity of MgO. On the other hand, as the Ce^{4+} ionic radius (1.01 Å) is larger than the radius of Mg^{2+} (0.65 Å), the peak shift may be caused by the insertion of Ce^{4+} ions to the crystal structure of Mg^{2+} causing the subsequent distortion of the crystal structure.

By increasing ceria concentration to 2.0–6.0 wt%, a strong peak at $2\theta = 28.5°$ and a number of weaker characteristic peaks of fluorite structured CeO_2 could be clearly detected. At this level of ceria loading, the primary diffraction peak of MgO was found to be 42.7° and 43.0° for Li/MgO/Ce2.0 and Li/MgO/Ce6.0, respectively. These values are closer to the normal diffraction angle observed for Li/MgO (43.2°). This suggests that the distortion of MgO structure became less obvious at the higher ceria loading. The formation of other types of mixed oxide was not observed in all the catalysts.

Fig. 2 shows the O 1s and C 1s X-ray photoelectron spectra of the Li/MgO based samples. The O 1s shows a dominant peak in the range of 531.3–531.7 eV (Peak B) and this can be unambiguously ascribed to O^{2-}. A shoulder peak emerging at lower energy of 529.2–529.7 eV (Peak A) is also clearly visible. The assignment of this shoulder peak

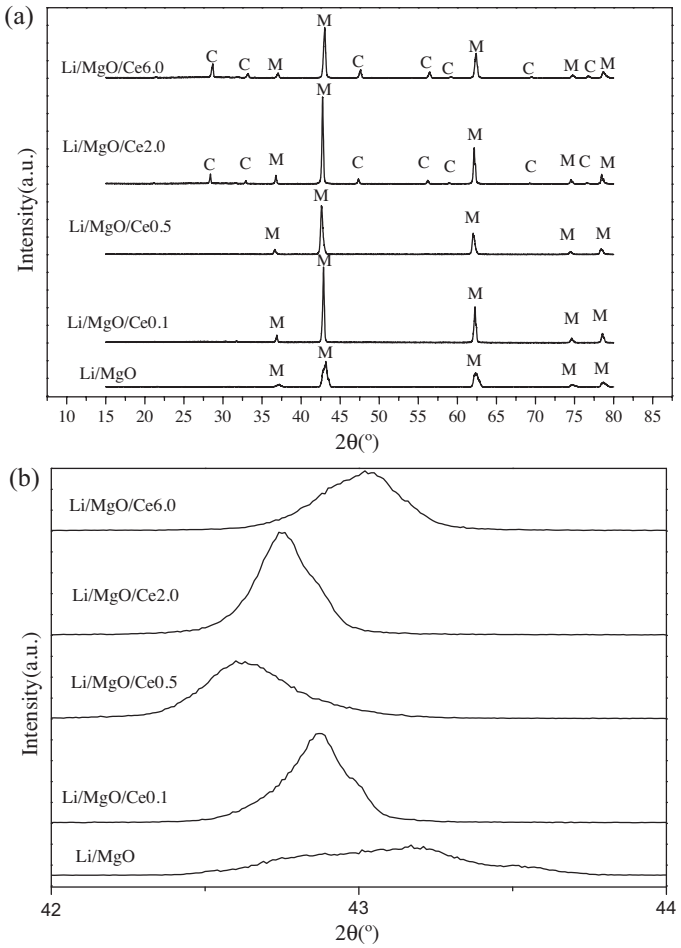

Fig. 1. (a) X-ray diffractograms of fresh catalysts. C: CeO_2, M: MgO; (b) the primary diffraction peak of MgO.

in the literature remains controversial as indicated by the various proposals reported. Nagaoka et al. [23] reported a binding energy of the shoulder peak, being ca. 2.0 eV higher than the O^{2-} peak for 10.0 wt% Li/MgO, and the shoulder peak was assigned to the oxygen from O^- and CO_3^{2-}. However, Aritani et al. [26] found a shoulder peak, ca. 2.0 eV lower than the O^{2-} peak for 2.5 wt% Li/MgO and it was assigned to lithium carbonate species. The result obtained in this study agrees well with the latter. However, as carbonate alone cannot account for the changing size of the shoulder peak, the shoulder peak observed was likely originated from O^- and CO_3^{2-} and the method suggested from Nagaoka et al. [23] was adopted to determine the surface O^-/O^{2-} atomic ratio.

Two C 1s peaks are observed and they are assigned to amorphous carbon at 285.0 eV (Peak C) and carbonate at 289.8 eV (Peak D) [27].

Table 2 shows the ratio of O^-/O^{2-} and the surface atomic concentration of ceria determined from XPS analysis. The ratio of O^-/O^{2-} increased from 0.31 to 0.54 at a ceria concentration of 0.5 wt% on Li/MgO. When ceria loading was increased further, this

Table 1
Surface area of fresh and used catalysts.

Sample	Specific surface area (m^2/g)	
	Fresh	Used[a]
Li/MgO	3.5	2.4
Li/MgO/Ce0.1	1.5	1.4
Li/MgO/Ce0.5	4.8	3.9
Li/MgO/Ce2.0	4.7	3.3
Li/MgO/Ce6.0	2.4	2.5

[a] After 6 h of reaction at 750 °C and a CH_4:O_2 ratio of 5:1.

Table 2
XPS data of Li/MgO based catalysts.

Sample	O 1s (O^-) B.E./e.V.	O 1s (O^{2-}) B.E./e.V.	O^-/O^{2-}	Ce %
Li/MgO	529.2	531.3	0.31	0.0
Li/Mg/Ce0.1	529.2	531.3	0.35	0.29
Li/MgO/Ce0.5	529.2	531.3	0.54	0.73
Li/MgO/Ce2.0	529.7	531.7	0.51	0.44
Li/MgO/Ce6.0	529.7	531.5	0.42	0.41

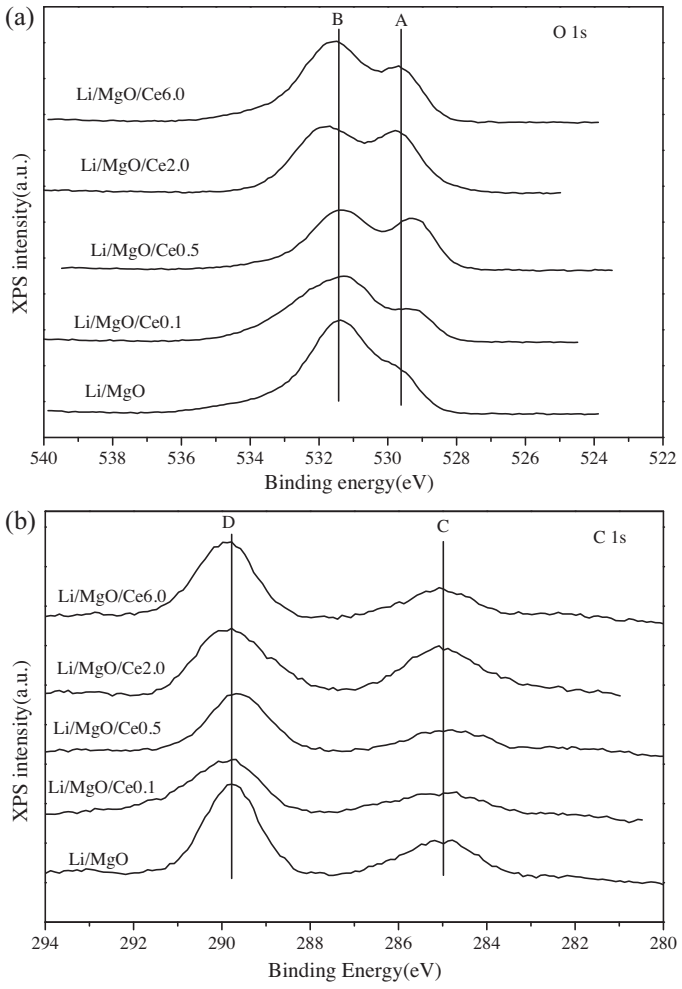

Fig. 2. XPS spectra over fresh Li/MgO based catalysts (a) O 1s and (b) C 1s.

ratio started to decrease. The surface atomic concentration of ceria showed a similar trend, indicating that less ceria became detectable on the surface when the ceria loading is higher than 0.5 wt%. This observation suggests that ceria could possibly be segregated at high ceria loadings resulting in poor dispersion of ceria species on the Li/MgO catalyst surface.

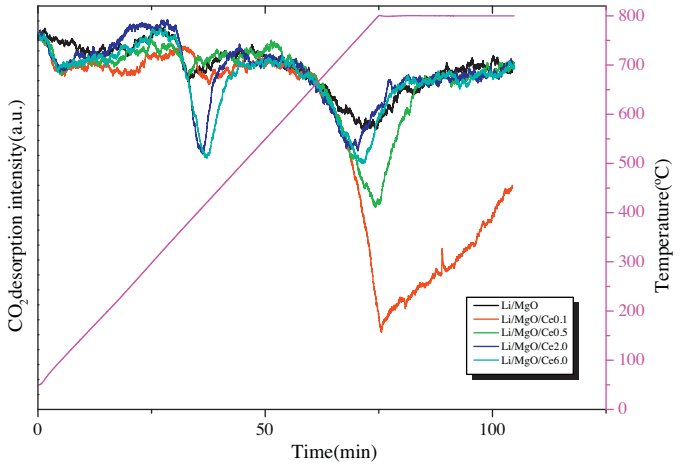

Fig. 3. CO_2 TPD spectra of fresh catalysts.

The CO_2 TPD profiles of the catalysts are given in Fig. 3. All samples showed similar desorption patterns and each gave two CO_2 desorption peaks. The first peak emerged in the temperature range of 400–420 °C and the second peak emerged in the temperature range of 770–800 °C. This suggests that there were at least two distinct sites for adsorbed CO_2 on the catalyst surface.

The desorption of CO_2 at higher temperature generally represents the presence of a stronger basic site [28]. It can be observed that both the high and low temperature desorption peaks of Li/MgO were weak. However, this changed with the amount of ceria added. The presence of ceria resulted in an increase in basic sites, either weak or strong depending on the concentration of ceria. Doping ceria at 0.1 wt% and 0.5 wt% substantially increased the response from the high temperature signal but no significant change was observed at the low temperature region. On the contrary, when the ceria loading was increased to 2.0 and 6.0 wt%, the response from the strong basic sites started to decrease accompanied by an increasing signal from the weak basic sites.

According to Choudhary and Rane [29], the basicity of catalysts, which can be interpreted as the electron pair donor strength, is attributed to the O^{2-} anions present on the surface. Therefore, the base strength of the surface sites is expected to vary with the effective charge of the O^{2-} anions and/or their effective coordination on the surface. Based on this result, it can be deduced that ceria could have modified the catalyst surface structure and the way CO_2 bound with the surface.

Fig. 4 presents the SEM images of Li/MgO and ceria doped samples. Unmodified Li/MgO particles generally have their sizes fall in the range of 20–40 nm. The Li/MgO/Ce0.5 appeared to be much larger in size than the unmodified Li/MgO with particles having round corners. Distinct particles exhibited a size in between 200 and 400 nm. Ceria particles were well dispersed on the outer surfaces of MgO. The Li/MgO/Ce6.0 also contained similar sized particles. However, particles were less distinct when compared to Li/MgO/Ce0.5 samples, and mostly fused structures were observed. Ceria particles can also be observed on the outer surface of the sample but seemed to be agglomerated, resulting in poor dispersion. This result agrees with the XPS analysis result discussed previously (Table 2), where an increase in ceria concentration resulted in poor dispersion of ceria on the surface.

3.2. Methane pulsing experiments

An absence of gaseous oxygen in the reaction zone is favourable for lowering the yield of CO_2, which is the oxidation product of methane and C_2 hydrocarbons, and consequently for improving the selectivity of C_2 hydrocarbons. Therefore it is desirable to limit the direct oxidation of methane by gaseous oxygen and help to improve C_2 selectivity in the OCM reaction by alternate feeding of gaseous oxygen and methane to the system. Since ceria has a relatively high oxygen storage capacity, its oxygen may be used to activate the methane molecules. In this case, the ceria promoted Li/MgO is a potential candidate to fulfil this role. In order to examine this hypothesis, the activity of Li/MgO/Ce0.5 in the absence of gaseous oxygen were investigated by passing a series CH_4 pulses of fixed-volume (0.5 ml) over the catalyst at 750 °C after oxygen pre-treatment.

Five pulses of CH_4 were injected and allowed to react over a fixed bed of Li/MgO/Ce0.5 catalyst. The results obtained (not shown here) indicate that neither C_2H_6 nor CO_2 were formed for any pulse of CH_4 injected. All other catalysts with higher ceria loadings showed a similar trend. This finding suggests that under the conditions, the oxygen stored in ceria does not act like gaseous oxygen and gaseous oxygen must be supplied in order to activate the methane molecules for the coupling reaction to take place on the surface of

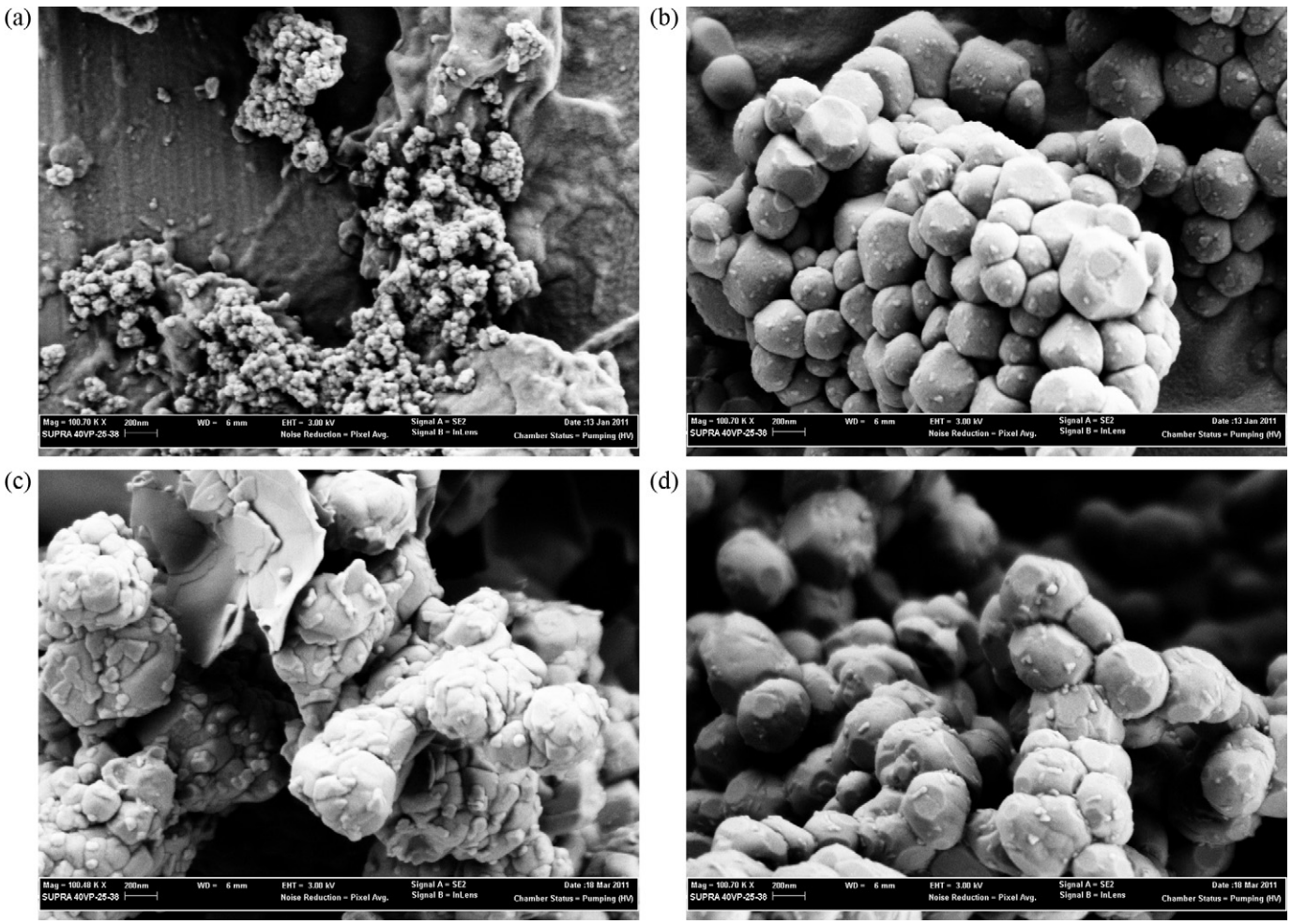

Fig. 4. Morphology of (a) Li/MgO; (b) Li/MgO/Ce0.5; (c) Li/MgO/Ce6.0; (d) used Li/MgO/Ce0.5 sample (after 6 h reaction at 750 °C and a CH_4:O_2 ratio of 5:1).

the catalyst. In this case, the ceria doped Li/MgO catalysts cannot work in a redox approach in the condition employed.

3.3. Catalytic activity

Fig. 5 shows the effect of ceria loading on the CH_4 and O_2 conversions, and C_2 selectivity measured after 6 h of reaction. It can be seen that the ceria loading has a strong effect on the catalyst activity. The addition of 0.1 wt% of ceria caused an increase in the steady-state methane conversion from 16.8% to 23.2%. The methane conversion reached a maximum value of 24.3% at a ceria loading range of 0.5–1.0 wt%. However, further increases in ceria loading decreased the CH_4 conversion to 18.3% at a ceria loading of 6.0 wt%.

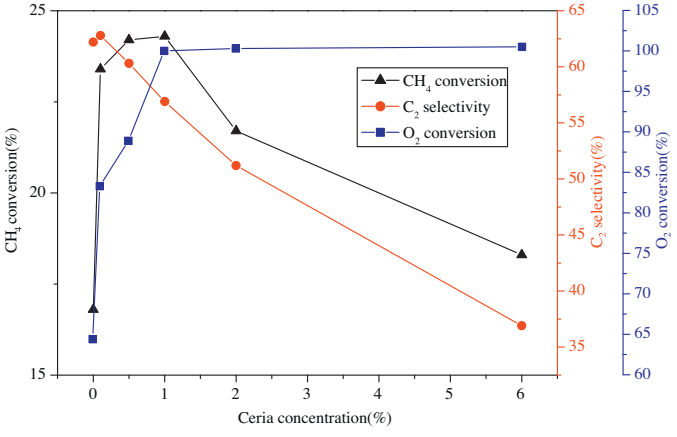

Fig. 5. Effects of ceria loading on CH_4 and O_2 conversion, and C_2 selectivity. Temperature: 750 °C, CH_4:O_2 = 5:1, mass: 450 mg, flow rate: 100 ml/min.

Li/MgO, Li/MgO/Ce0.1 and Li/MgO/Ce0.5 gave similar C_2 selectivity of above 60%. However, the selectivity decreased significantly when the ceria loading was increased further. It was noted that O_2 conversion reached higher values in the presence of ceria. At a 6.0 wt% loading of ceria, the C_2 selectivity decreased to around 35%. A detailed analysis of carbon balance for the gas produced is given in Table 3. It can be observed that CO_2 was the dominant product of full oxidation while at the same time, small amount of CO was also produced. It can be seen that the addition of ceria changed the C_2H_4/C_2H_6 ratio. The C_2H_4/C_2H_6 ratio increased from 0.56 for Li/MgO to 0.92 for Li/MgO/Ce0.5. Further increases in ceria loading increased significantly the production of CO_2 and lowered the C_2H_4/C_2H_6 ratio.

Table 3
Effect of ceria loading on carbon balance of OCM products in the gas phase.

	CO (%)	CO2 (%)	C2H4 (%)	C2H6 (%)	C2H4/C2H6 ratio
Li/MgO	3	35	22	40	0.56
Li/Mg/Ce0.1	2	35	28	34	0.83
Li/MgO/Ce0.5	2	38	29	31	0.92
Li/MgO/Ce2.0	3	46	23	28	0.82
Li/MgO/Ce6.0	6	57	12	25	0.47

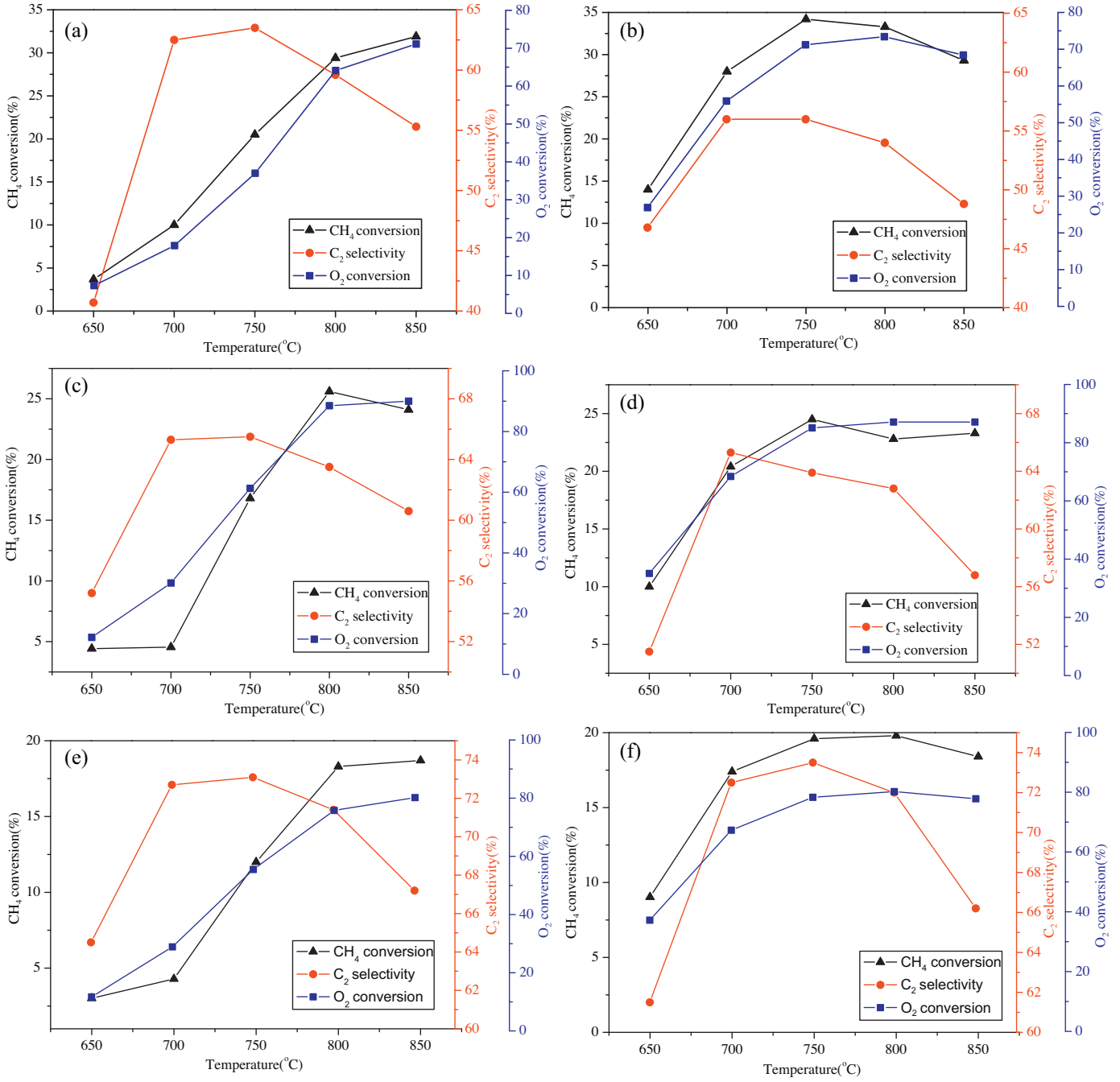

Fig. 6. Catalytic testing results of Li/MgO and Li/MgO/Ce0.5. (a) Li/MgO at CH_4:O_2 = 3:1; (b) Li/MgO/Ce0.5 at CH_4:O_2 = 3:1; (c) Li/MgO at CH_4:O_2 = 5:1; (d) Li/MgO/Ce0.5 at CH_4:O_2 = 5:1; (e) Li/MgO at CH_4:O_2 = 7:1; (f) Li/MgO/Ce0.5 at CH_4:O_2 = 7:1.

As given in Table 1, the used samples show a slight decrease of surface area when compared to the fresh samples. After 6 h of reaction, the surface area of Li/MgO/Ce0.5 decreased from 4.8 m^2/g to 3.9 m^2/g and no decrease of OCM activity can be observed. XRD analysis of used Li/MgO/Ce0.5 (not shown here) also displays similar diffraction patterns to the fresh sample, which confirms the absence of any new phase in the used catalyst. Little morphological change can be observed for used Li/MgO/Ce0.5 catalysts (Fig. 4(d)). All of these provide strong evidence that the Li/MgO/Ce0.5 is a stable catalyst for the coupling reaction.

Fig. 6 compares the coupling performance of Li/MgO and Li/MgO/Ce0.5 under various reaction temperatures and CH_4:O_2 ratios. Li/MgO/Ce0.5 was selected for comparison because it showed the highest CH_4 conversion and C_2 selectivity among all ceria promoted catalysts employed in the current study (Fig. 5).

Increasing the CH_4:O_2 ratio resulted in the decrease of methane conversion and an increase in C_2 selectivity. This trend agrees well with the results reported by others [28,30]. For example, at 750 °C and a CH_4:O_2 ratio of 3:1, the measured methane conversion for Li/MgO/Ce0.5 is 34.5%, and this decreased to 19.8% at a CH_4:O_2 ratio of 7:1, while the C_2 selectivity increased from 55.0% to 73.0%. This is because in an oxygen lean environment, the reaction between $CH_3^{\bullet}$ and O_2 to produce methoxy species decreases, which leads to a lower production of CO_x.

At a CH_4:O_2 ratio of 3:1, the Li/MgO/Ce0.5 catalyst showed a lower C_2 selectivity when compared to Li/MgO (for example 55% for Li/MgO/Ce0.5 and 65% for Li/MgO at 750 °C, given in Fig. 6(a) and

(b)). When the CH_4:O_2 ratio was increased to 7:1, the selectivity of Li/MgO/Ce0.5 catalyst reached ca. 72% and was similar to that of Li/MgO (Fig. 6(e) and (f)).

Li/MgO and Li/MgO/Ce0.5 responded differently to changes in reaction temperature. For Li/MgO, increasing temperature resulted in increasing CH_4 conversion while the maximum C_2 selectivity occurred at 750 °C. For Li/MgO/Ce0.5, the CH_4 conversion reached a maximum at 750 °C and it decreased at higher reaction temperatures (850 °C). Similar to Li/MgO, the selectivity of Li/MgO/Ce0.5 reached a maximum at between 700 and 750 °C.

The promoting effect of ceria was more pronounced at temperatures <800 °C. At 650 °C and a CH_4:O_2 ratio of 3:1, the Li/MgO showed a CH_4 conversion of less than 5.0%, while the Li/MgO/Ce0.5 catalyst gave a CH_4 conversion of 15.0% (Fig. 6(a) and (b)). However, there was less promoting effect of ceria at 850 °C and the methane conversion of Li/MgO/Ce0.5 was close to that of Li/MgO. At a CH_4:O_2 ratio of 7:1, both catalysts gave a methane conversion of ca. 18% (Fig. 6(e) and (f)). The results also show that there is a significant decrease in temperature for onset activity when promoted with 0.5 wt% of ceria, i.e. 700–800 °C for Li/MgO and 650–750 °C for Li/MgO/Ce0.5.

4. Discussion

The surface basicity/acidity has been suggested to contribute to the activity and selectivity of OCM catalysts [29]. From the CO_2 desorption results (Fig. 3), it seems that strong basic sites are associated with the improvement observed in methane conversion while the weak basic sites are associated with low C_2 selectivity. The increase of strong basic sites in the 0.1 wt% and 0.5 wt% ceria loaded catalysts resulted in an improvement in methane conversion, while a decrease in strong basic sites and an increase in weak basic sites in the 2.0 wt% and 6.0 wt% ceria loaded catalysts resulted in low methane conversion and poor selectivity. This in general agrees with the mechanism suggested by Choudhary that methane activation occurs via heterolytic cleavage on low-coordination basic sites [29]. However, a direct correlation between the OCM selectivity and activity of the ceria doped catalysts and surface basicity cannot be obtained. For example, there was not much improvement in methane conversion with the 0.1 and 0.5 wt% ceria promoted catalysts while there is a significant decrease of strong basicity site between them. Analysis of the data from different approaches is needed.

The selectivity and activity of the OCM catalysts were in general related to the nature of the oxygen species on the surface, which in turn, is determined largely by the electronic properties of the solid catalyst [3]. For Li/MgO, it is generally accepted that $[Li^+O^-]$ is the active site for OCM, and is responsible for the generation of $CH_3^\bullet$ radicals by abstracting hydrogen from methane [31]. The widely accepted mechanism for the regeneration of activate sites as suggested by Lunsford [31] is described by Reactions (1)–(3):

$$CH_4 + [Li^+O^-] \rightarrow CH_3^\bullet + Li^+OH^- \quad (1)$$

$$2Li^+OH^- \rightarrow Li^+O^{2-} + H_2O + Li^+\square \quad (2)$$

$$Li^+O^{2-} + Li^+\square + (1/2)O_2 \rightarrow 2[Li^+O^-] \quad (3)$$

where □ is the oxygen vacancy.

Ceria is considered a poor OCM catalyst having low C_2 selectivity but exhibits high activity towards CH_4 oxidation and production of CO_x. On one side, the oxides in the lanthanide series that exhibit multiple cationic oxidation states (CeO_2, Pr_6O_{11}, and Tb_4O_7) are not effective in generating gas-phase $CH_3^\bullet$ radicals. On the other side, these oxides react efficiently with the $CH_3^\bullet$ radicals to produce methoxide species [7]. Thus, even if CH_4 is activated to form $CH_3^\bullet$ on these oxides, there is a good chance that these short-life radicals would be oxidized to CO_x through the methoxide pathway (Reaction (5)) prior to coupling (Reaction (4)). As shown in the present work, depending on the ceria loading and the reaction conditions, such as reaction temperature and CH_4:O_2 ratio, ceria showed a significant promoting effect for Li/MgO during the OCM process.

$$CH_3^\bullet + CH_3^\bullet \rightarrow C_2H_6 \quad (4)$$

$$CH_3^\bullet + O_2 \rightarrow CH_3O^\bullet \rightarrow CO_x \quad (5)$$

The promoting effect occurred predominantly at low ceria loadings (<1.0 wt%) where most of the ceria is inserted into the lattice structure of Li/MgO. With higher ceria loadings (2.0 wt% and 6.0 wt%), it is likely that segregation of ceria may occur, resulting in less ceria being inserted into the lattice structure of Li/MgO. This was supported by XRD (Fig. 1) and SEM (Fig. 4) analyses. This segregated state of ceria is thought to behave as the bulk ceria and improve the catalytic reaction between methane and O_2 in producing CO_x. The increase in CH_4 and O_2 consumption was an indication of methane oxidation and CO_x formation, and consequently lowered C_2 selectivity (Fig. 5). Voskresenskaya et al. concluded that the maximum in activity occurs within the range of solid solution formation for promoted catalysts and catalysts with high promoter content may form an active phase consisting of a compound of the promoter itself [32]. This finding agrees very well with the results presented in this study.

It has been shown that doping materials with cations of different valences from that of host ion is a promising method for creating defects [32]. In this study, the oxygen defect sites are expected to form when ceria is inserted into the structure of Li/MgO. The change in distribution of oxygen species on the surface is revealed in the XPS results. As shown in Table 2, the $[O^-]/[O^{2-}]$ ratio reached a maximum for Li/MgO/Ce0.5 and this ratio started to decrease as ceria loading increased. From this finding, it can be deduced that ceria at this loading could improve the formation of defect sites useful for OCM. The results obtained from XRD also suggest the evolution of structural defects after the introduction of ceria (Fig. 1). At the same time, high methane conversion was observed for the Li/MgO/Ce0.5 (Fig. 5), which further confirmed that $[Li^+O^-]$ is mainly responsible for methane activation. However, the differences in surface area between the samples tested were small so a significant surface area effect was hard to ascertain.

As suggested by Zhang et al., the presence of a transition metal ion dopant having multivalent states could act as a charge carrier and therefore assists the charge transfer processes within the catalyst [3]. When the Li/MgO was doped with ceria, alternative pathways for the formation of $[Li^+O^-]$ active site may be possible. The reaction mechanism developed by Bartsch et al. [33] has been modified to describe mechanism through charge transfer in the ceria promoted Li/MgO system (Fig. 7).

Trovarelli [14] proposed that the adsorption of gaseous O_2 on reduced ceria surface would lead to the incorporation of oxygen into the lattice through reactions (6)–(9) via the capturing of the electron as a result of the separation of a positive hole (h^+) and negative electron (e^-) charge pair on the catalyst surface [34]. During this oxygen incorporation process, reaction (10) which represents the formation of $[Li^+O^-]$ site and the reduction of Ce^{4+} to Ce^{3+} could be possible.

$$O_{(ads)}^- + Ce^{4+} + [Li^+e^-h^+] \rightarrow Ce^{3+} + [Li^+O^-] + h^+ \quad (10)$$

This reaction provides an alternative pathway for the formation of the $[Li^+O^-]$ active site with an extra hole formed through the charge transfer between Ce^{4+} and Ce^{3+}. The O^- species was reported by Lecomte et al. [35] to be present on the surface of CeO_2/Al_2O_3 samples and Dedov [18] also reported that oxygen could be activated directly to produce O^- species when the gaseous oxygen

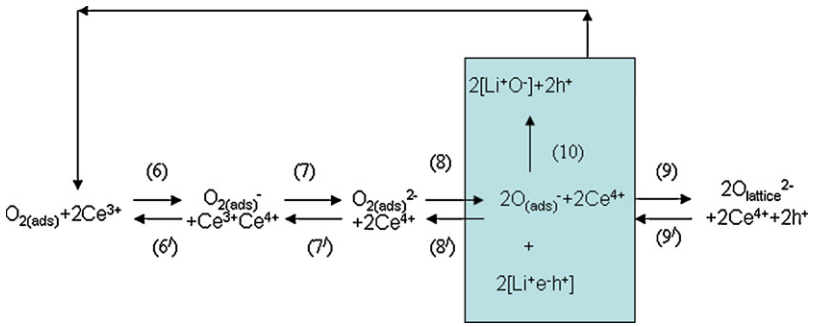

Fig. 7. A proposed reaction mechanism of $[Li^+O^-]$ formation over ceria promoted Li/MgO catalyst, where e^-: electron, h^+: hole with positive charge.

was brought into contact with ceria. However, ceria gave poor C_2 selectivity, which suggested that the O^- species formed through reactions (6)–(8) was unstable and was easily incorporated into the lattice of ceria through reaction (9) for the oxidation reaction. On the other hand, the O^- species on supported ceria is stabilised as a form of $[Li^+O^-]$ as per reaction (10) and hence the OCM activity of ceria promoted Li/MgO catalysts is improved.

Reaction (9) where the oxygen is incorporated into the lattice of ceria and reaction (10) may be competing, depending on the reaction temperature and O_2 concentration in the gas phase. It has been shown that Li/MgO/Ce0.5 showed an improved activity at lower temperature compared to Li/MgO. This alludes to the possibility of $[Li^+O^-]$ site formation through reaction (10) at lower temperatures as compared to the active site formation given by reactions (1)–(3). On the other hand, increasing reaction temperature and oxygen concentration were favourable for reaction (9), resulting in less $[Li^+O^-]$ site formation and a decrease of methane conversion and C_2 selectivity. This agrees with the result (Fig. 6) where both CH_4 conversion and C_2 selectivity decreased at high temperature (850 °C) and low CH_4/O_2 ratio (3:1) for Li/MgO/Ce0.5.

Despite the improved methane conversion at 0.5–1.0 wt% ceria loadings, little improvement in C_2 selectivity was observed (Fig. 5). One reason is that besides acting as a methane activator, the oxygen species, including $[Li^+O^-]$ and lattice oxygen O^{2-}, may also act as oxidants for the $CH_3^\bullet$ radicals to produce CO_x. As Zhang et al. [3] pointed out, an ideal OCM catalyst should possess a high capacity to transform oxygen species into lattice oxygen, as the lattice oxygen is less oxidizing than the active oxygen species (e.g. O^-). It should be pointed out here that the function of the lattice oxygen in ceria and in magnesium oxide is different. It is believed that lattice oxygen in ceria favours the full oxidation of methane while lattice oxygen in MgO is relatively less oxidative and favours formation of C_{2+} hydrocarbons instead of carbon oxides. Thus, the lack of improvement observed for C_2 selectivity could be caused by the small change in the transfer of oxygen species into MgO lattice oxygen with the introduction of ceria. This can be explained by the proposed mechanism that the migration of oxygen into ceria through reactions (6)–(9) is anticipated to be much faster than the transfer into MgO due to the excellent redox properties of ceria.

Ceria doped Li/MgO catalysts did not convert CH_4 into C_2 hydrocarbons in the absence of gaseous oxygen. As indicated by reactions (1)–(3), the active site $[Li^+O^-]$ formation is impossible on these materials without gaseous oxygen. It can be deduced that the reverse reaction (9′) did not occur when methane was used as the reducing agent. In this case, no active site can be formed in the absence of gaseous oxygen through reaction (10). Our conclusion is opposite to that of Nagaoka et al. [23] who concluded that O^{2-} from the complex oxide containing Sn is another type of active centre for OCM and performs the redox cycle between Sn^{4+} and Sn^{2+} in a Sn promoted Li/MgO catalyst. This discrepancy is due to a difference in the oxidation ability of O^{2-} species between ceria and SnO_2. As mentioned above, O^{2-} in ceria cannot act as the active site for C_2 formation. Therefore the mechanism that Nagaoka et al. [23] postulates, that the reaction proceeds by a redox cycle with O^{2-} as the activate site, cannot be used to describe the ceria doped Li/MgO catalysts in this study.

In another study, Otsuka [36] reported that methane can react with CeO_2 directly to produce synthesis gas in a H_2/CO ratio of 2:1. In this work, the lack of formation of H_2, as indicated by $m/z = 2$ and CO, as indicated by $m/z = 28$, in the pulse study suggested that lattice oxygen could not facilitate the oxidation of methane. This may be partly due to the slow reaction rate of the lattice oxygen in ceria with CH_4 at 750 °C. Another possibility is that a low gas hourly space velocity (large mass) is normally required for the reaction. Compared to the work of Otuska [36], the gas hourly space velocity in our pulse reaction was one order faster, which may also affect the CH_4 conversion.

5. Conclusions

The ceria loading has a great effect on the Li/MgO properties and its OCM activity. While the ceria loading does not significantly alter the surface area of catalysts, XRD results suggested that low concentrations of ceria can properly insert into the MgO structure, resulting in a distortion of its structure and the formation of surface defects. XPS results confirmed the existence of defect site of O^- species. A maximum $[O^-]/[O^{2-}]$ ratio occurs at 0.5 wt% ceria loading.

The 0.5–1.0 wt% ceria doped Li/MgO catalyst shows an improved methane conversion for the OCM reaction, particularly at lower temperatures when compared to the undoped Li/MgO material. No improvement in C_2 selectivity was observed with the addition of ceria. High ceria loading (>2.0 wt%) resulted in significantly lower C_2 selectivity. High reaction temperatures (>800 °C) and decreased CH_4:O_2 ratios (7:1 to 3:1) caused a decrease of methane conversion and C_2 selectivity for Li/MgO/Ce0.5. The ceria doped catalyst does not show any C_2 productivity in the absence of gaseous oxygen and it is concluded that this system cannot facilitate OCM using lattice oxygen stored in the catalyst structure. A new pathway for the active site formation through the electron transfer between $Ce^{4+}/Ce^{3+}$and Li/MgO is proposed and accounts for the doped ceria effects on the catalyst performance. Further investigations are being conducted to address the long-term stability of these catalysts.

Acknowledgment

We acknowledge the assistance of Dr. Bill Gong from the University of New South Wales in conducting the XPS analysis.

References

[1] A. Holmen, Catal. Today 142 (2009) 2–8.
[2] M. Reisch, C&EN 85 (2007) 12.
[3] Z.L. Zhang, X.E. Verykios, M. Baerns, Catal. Rev.-Sci. Eng. 36 (1994) 507–556.
[4] G.E. Keller, M.M. Bhasin, J. Catal. 73 (1982) 9–19.
[5] T. Ito, J.X. Wang, C.H. Lin, J.H. Lunsford, J. Am. Chem. Soc. 107 (1985) 5062–5068.
[6] S. Kuś, M. Otremba, M. Taniewski, Fuel 82 (2003) 1331–1338.
[7] Y. Tong, M.P. Rosynek, J.H. Lunsford, J. Phys. Chem. 93 (1989) 2896–2898.
[8] E.V. Kondratenko, M. Baerns, Oxidative coupling of methane, in: G. Ertl, H. Knözinger, F. Schüth, J. Weitkamp (Eds.), Handbook of Heterogeneous Catalysis, Wiley-VCH, Weinheim, 2008, pp. 3010–3023.
[9] G.D. Moggridge, J.P.S. Badyal, R.M. Lambert, J. Catal. 132 (1991) 92–99.
[10] Z. Fakhroueian, F. Farzaneh, N. Afrookhteh, Fuel 87 (2008) 2512–2516.
[11] S.J. Korf, J.A. Roos, N.A. De Bruijn, J.G. van Ommen, J.R.H. Ross, Appl. Catal. 58 (1990) 131–146.
[12] S.J. Korf, J.A. Roos, L.J. Veltman, J.G. van Ommen, J.R.H. Ross, Appl. Catal. 56 (1989) 119–135.
[13] A.M. Gaffney, C.A. Jones, J.J. Leonard, J.A. Sofranko, J. Catal. 114 (1988) 422–432.
[14] A. Trovarelli, Catal. Rev.-Sci. Eng. 38 (1996) 439–520.
[15] J.G.A. Pacheco Filho, J.G. Eon, M. Schmal, Catal. Lett. 68 (2000) 197–202.
[16] Z.L. Zhang, M. Baerns, J. Catal. 135 (1992) 317–320.
[17] S.M.K. Shahri, A.N. Pour, J. Nat. Gas Chem. 19 (2010) 47–53.
[18] A.G. Dedov, A.S. Loktev, I.I. Moiseev, A. Aboukais, J.-F. Lamonier, I.N. Filimonov, Appl. Catal. A 245 (2003) 209–220.
[19] Y.L. Bi, K.J. Zhen, Y.T. Jiang, C.W. Teng, X.G. Yang, Appl. Catal. A 39 (1988) 185–190.
[20] S. Bartsch, H. Hofmann, Catal. Today 6 (1990) 527–534.
[21] R.L.P. Gonçalves, F.C. Muniz, F.B. Passos, M. Schmal, Catal. Lett. 135 (2010) 26–32.
[22] V.R. Choudhary, S.T. Chaudhari, M.Y. Pandit, J. Chem. Soc., Chem. Commun. 17 (1991) 1158–1159.
[23] K. Nagaoka, T. Karasuda, K. Aika, J. Catal. 181 (1999) 160–164.
[24] L. Leveles, K. Seshan, J.A. Lercher, L. Lefferts, J. Catal. 218 (2003) 307–314.
[25] C. Trionfetti, I.V. Babich, K. Seshan, L. Lefferts, Appl. Catal. A 310 (2006) 105–113.
[26] H. Aritani, H. Yamada, T. Nishio, T. Shiono, S. Imamura, M. Kudo, S. Hasegawa, T. Tanaka, S. Yoshida, J. Phys. Chem. B 104 (2000) 10133–10143.
[27] X.D. Peng, D.A. Richards, P.C. Stair, J. Catal. 121 (1990) 99–109.
[28] A.M. Maitra, Appl. Catal. A 194 (1993) 11–59.
[29] V.R. Choudhary, V.H. Rane, J. Catal. 130 (1991) 411–422.
[30] H. Zanthoff, M. Baerns, Ind. Eng. Chem. Res. 29 (1990) 2–10.
[31] J.H. Lunsford, Angew. Chem. Int. Ed. Engl. 34 (1995) 970–980.
[32] E.N. Voskresenskaya, V.G. Roguleva, A.G. Anshits, Catal. Rev.-Sci. Eng. 37 (1995) 101–143.
[33] S. Bartsch, J. Falkowski, H. Hofmann, Catal. Today 4 (1989) 421–431.
[34] J.L. Dubois, C.J. Cameron, Appl. Catal. A 67 (1990) 49–71.
[35] J.J. Lecomte, P. Granger, L. Leclercq, J.F. Lamonier, A. Aboukaïs, G. Leclercq, Colloid Surf. A 158 (1999) 241–247.
[36] K. Otsuka, Y. Wang, E. Sunada, I. Yamanaka, J. Catal. 175 (1998) 152–160.